Enhanced magneto-optical effects in hybrid Ni-Si metasurfaces EP

M. G. Barsukova, A. I. Musorin (iD), A. S. Shorokhov (iD), and A. A. Fedyanin (iD)

COLLECTIONS

EP   This paper was selected as an Editor's Pick

View Online   Export Citation   CrossMark

ARTICLES YOU MAY BE INTERESTED IN

Low-loss fiber-to-chip couplers with ultrawide optical bandwidth
APL Photonics **4**, 010801 (2019); https://doi.org/10.1063/1.5064401

Realizing $Q >$ 300 000 in diamond microdisks for optomechanics via etch optimization
APL Photonics **4**, 016101 (2019); https://doi.org/10.1063/1.5053122

Directional light emission enhancement from LED-phosphor converters using dielectric Vogel spiral arrays
APL Photonics **3**, 126103 (2018); https://doi.org/10.1063/1.5052637

Enhanced magneto-optical effects in hybrid Ni-Si metasurfaces (EP)

M. G. Barsukova, A. I. Musorin, (iD) A. S. Shorokhov, (iD) and A. A. Fedyanin[a] (iD)

AFFILIATIONS

Faculty of Physics, Lomonosov Moscow State University, Moscow 119991, Russia

[a]Author to whom correspondence should be addressed: fedyanin@nanolab.phys.msu.ru

ABSTRACT

The multifold enhancement of the Faraday effect induced by magnetic dipole and Voigt effect amplification due to electric dipole Mie resonances of the magnetophotonic metasurface is demonstrated. The values of the magneto-optical responses up to 0.8° and 0.5% are experimentally observed for the metasurface with an ultrathin ferromagnetic layer. The results can be used for the development of novel active magnetophotonic metadevices.

The primary goal of magneto-optics (MO) is to manipulate the light properties by applying an external magnetic field through combining two areas of physics: magnetism and optics. Spin-orbit interaction is responsible for MO effects, which are widely used to understand the internal structure of magnetic materials, elementary excitations, and motion of magnetic domain walls.[1] This knowledge allows one to understand the mechanisms of magnetism. The driving force of MO effects is the Lorentz force[2] being considerably smaller than the electric one accounting for weak MO effects at the optical frequencies.[2] Thus, these effects need to be enhanced to be successfully implemented to photonic technologies for controlling light properties via an external magnetic field.

During the past 30 years, various methods have been discovered to boost the magneto-optical response. One of the first mechanisms for MO enhancement is exciting the local plasmon resonance in magnetic nanoparticles made of Fe_3O_4.[3] Many modifications have been proposed to localize light at the nanoscale.[4] For example, combination of noble and magnetic materials in nanoparticles,[5] embedding gold nanoparticles in magnetic dielectric,[6,7] and ferromagnetic nanodisks[8,9]. The enhancement of magneto-optical effects can be reached via the excitation of surface plasmon-polaritons.[10] The external magnetic field in a transverse geometry modulates the wave vector of the surface plasmon-polaritons leading to the modification of an intensity magneto-optical effect.[11]

Localizing this surface wave near the magnetic dielectric can also enhance the polarization magneto-optical effect.[12] The modification of magneto-optical spectra was demonstrated in case the localized plasmons were hybridized with propagating surface plasmon waves.[13]

Another mechanism to enhance MO is a slow light regime due to a multibeam interference in magnetophotonic crystals.[14] These structures are advantageous as they are made of all-dielectric materials without metal inclusions and demonstrate a high value of Faraday rotation as well as transmittance.[15,16] The intriguing results are observed in magnetophotonic crystals when the optical Tamm or Bloch surface states are excited.[17-20] Recently, a novel method has been demonstrated to enhance the intensity magneto-optical effect.[21] The excitation of magnetic dipole Mie resonance in far-standing silicon nanodisks covered with the thin nickel film leads to an increased magneto-optical response. The basic idea to enhance MO effects is to concentrate the light energy inside a magnetic material or on its edge. The phenomenon of MO effect enhancement is widely used for various applications in optical modulators,[22] filters,[23] isolators,[24] sensors,[25,26] and lasers.[27] Another possible application is the magneto-optical data writing, where powerful femtosecond laser pulses can be used for magnetic order manipulating in gyrotropic materials.[28,29] These pulses result in demagnetization processes or magnetization reversal because of a strong excitation of the electrons and spins of the system. Structures with

different kind of optical resonances are used to decrease the radiation fluence for magnetization switching and to reduce the reversed magnetization area.[30] Nanoparticles with Mie resonances can be a new way not only to decrease the laser power required for switching but to generate a high-magnitude static magnetic field at the nanoscale as well. This possibility has been already demonstrated in theory.[31] More-over, ultrafast magneto-optics allows one to control the polarization state inside a single femtosecond laser pulse[32] or to modulate the shape of the laser pulse by nanostructured magneto-optical materials when an external magnetic field is switched on.[33]

Modern photonics considers metasurfaces as a promising approach to implement advances of fundamental science in real life.[34,35] They are planar subwavelength arrays of ordered nanoparticles–meta-atoms, which are able of manipulating the amplitude and phase of light at the nanoscale ensured by their resonant nature.[36,37] A number of static[38–40] and dynamic[41–43] configurations have been devised. These structures can concentrate light to form special modes corresponding to various resonances. In the context of magneto-optics, such structures can help to boost MO effects. Some progress has already been made in this direction by numerical simulations.[44,45] In this work, we take a further step toward combining metasurfaces with magneto-optical media (see Fig. 1) and experimentally show the Faraday effect enhancement in magnetophotonic metasurfaces.

The magnetophotonic metasurface is made up of a square lattice of hydrogenated amorphous silicon (a-Si) nanodisks placed on a transparent silica substrate and covered with a thin film of nickel (Ni). We analyze, both numerically and experimentally, the optical and magneto-optical spectra of such structures. The shape, diameter, height of the nanoparticles, and the array period are optimized by numerical simulations to control the position of the two fundamental Mie-type resonances in the visible and near-IR spectral ranges. All numerical and experimental results are presented for the sample comprising the array of silicon nanodisks with diameter d = 170 nm, height h = 220 nm, and lattice spacing a = 400 nm covered with a 5-nm-thick Ni film [see Fig. 1(a)]. The lattice spacing a of the array is chosen to eliminate the contribution

of diffraction and to increase the interparticle coupling. Since nickel has a high magnetic activity, it is added to the structure to achieve the magneto-optical response. The thickness of the nickel layer is optimized to avoid considerable optical losses as well as to achieve sufficient magneto-optical response. High efficiency and low losses of the aforementioned structure have been proven by corresponding numerical calculations. We use the normal incidence illumination in experiments and numerical simulations–the direction of a light wave vector is along the Z-axis and polarization is along the X-axis [see Fig. 1(a)].

Magnetic properties of the sample are characterized by vibrating sample magnetometry technique [see Fig. 1(b)]. Two magnetic hysteresis loops are measured. The first one is the in-plane configuration (red color on the figure) when an external magnetic field is applied parallel to the sample surface–along the Y-axis. This configuration is used for Voigt or transverse magneto-optical Kerr effects. The other configuration is the out-of-plane case (blue color on the figure) when an external magnetic field is applied perpendicularly to the sample surface–along the Z-axis. This configuration is used for the Faraday effect or polar magneto-optical Kerr effect measurements. The saturation field is approximately 1 kOe. Values of magnetization saturation are 35 μemu for in-plane configuration, while it is 10 μemu for out-of-plane configuration.

Numerical calculations are performed using the finite-difference time-domain (FDTD) technique in the Lumerical FDTD Solutions software (see Appendix A). In experiments and numerical simulations, we use the normal incidence illumination and two types of transmission configuration: (1) in the Faraday configuration, we apply an external magnetic field perpendicular to the sample surface and parallel to the light wave vector–along the Z-axis; (2) in the Voigt configuration, we apply an external magnetic field along the sample surface and perpendicular to the light wave vector and polarization–along the Y-axis.

The Faraday rotation spectra are measured with the polarization-sensitive technique (see Fig. 2). A near-IR Ti:sapphire laser is used as a light source in CW mode with an average intensity of 400 mW and tunability wavelength range from 760 to 810 nm. The linearly polarized light is focused at a normal incidence to the sample with a beam diameter
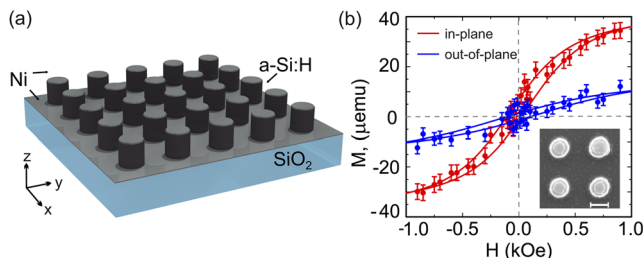

FIG. 1. (a) Schematic illustration of the magnetophotonic metasurface composed of Si nanodisks supporting magnetic Mie-type resonances. Disks are covered by a 5-nm-thick Ni film. (b) Magnetic hysteresis loops (dots—experiments and curves—fits) of the sample: in-plane (red) and out-of-plane (blue) configurations. The inset shows the SEM image of the sample. The scale bar is 200 nm.
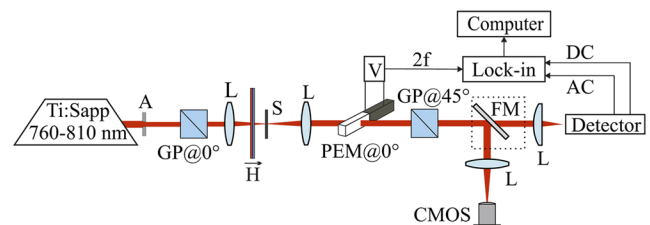

FIG. 2. Experimental setup for the Faraday rotation measurements. Ti:Sapp—titanium-sapphire laser; A—iris aperture; GP—Glan-Taylor polarizers; L—lenses; H—permanent magnetic field source; S—sample; PEM—photoelastic modulator; FM—flipping mirror; and CMOS—camera.

of approximately 100 μm in the sample plane, and then it passes through a photo-elastic modulator and a 45°-oriented Glan-Taylor prism, which converts the polarization modulation to the light intensity modulation. The sample is placed in the vicinity of a permanent magnetic field of 1 kOe oriented parallel to the light propagation direction.

Figure 3(a) shows experimental (curve with dots) and numerical (solid curve) Faraday rotation spectra. The spectra show a resonant enhancement of the MO effect in the vicinity of the magnetic dipole Mie-type resonance of Si nanodisks, while the spectrum of a reference flat Ni film (purple dots) does not have any peculiarities. The enhancement of the Faraday effect is approximately 10 times larger in comparison with the reference Ni film. These results are confirmed by numerical calculations [see Fig. 3(b)]. Since the spectrum of the MO response of the sample has resonant features in comparison with the unstructured nickel film, the enhancement of the magneto-optical response of the structure and the excitation of magnetic dipole resonance in a silicon nanodisk are in direct correlation. The discrepancies in Faraday rotation values can be explained by mismatch of dispersion data of non-diagonal elements of the nickel permittivity tensor. These data are taken from the literature[46] for calculations and may differ for the real sample.

We observe two dips in transmission spectrum, which correspond to the electric dipole (ed) Mie resonance of Si nanodisks at 675 nm and magnetic dipole (md) resonance at the wavelength of 770 nm [see Fig. 3(b)]. A strong

Faraday effect is observed just near the md mode. The resonance excitation is confirmed by numerical simulations [see Figs. 3(c)–3(f)]. Colormaps (c) and (e) show local electric field distribution, while (d) and (f) show local magnetic field distribution for electric and magnetic dipole resonances, respectively. The values of the electric field are almost equal for both types of resonances; however, the magnitude of the magnetic field is several times larger in magnetic dipole mode in comparison with electric dipole mode.

To confirm a correlation between the MO enhancement and magnetic dipole resonance excitation in the hybrid metasurface, we perform the proof-of-principle studies in the Voigt configuration. The experimental setup (see Fig. 4) used for measurements of the optical and magneto-optical spectra in the Voigt configuration is similar to the one used in Ref. 21. The light source is a halogen lamp, the radiation of which, passing through a monochromator with a spectral resolution of 3 nm, is collected by a collimating system of lenses in a beam with an aperture of 150 μm. The linearly polarized radiation after passing through the Glan-Taylor polarizer is focused on the sample surface with a beam diameter of 100 μm at a normal incidence. The light transmitted through the sample is collected to the photomultiplier tube through an optical fiber. A lock-in amplifier is used at an optical chopper's frequency of 113 Hz to detect the signal. The magneto-optical measurements are carried out without a chopper. The reference frequency of the lock-in amplifier is set at the double frequency of the external AC 0.5 kOe magnetic field (2f = 234 Hz). AC magnetic field is being generated by home-build Helmholtz coils. An absence of the analyzer in this scheme allows us to use the lamp as a source instead of the laser because the light intensity is enough to detect the MO effect.

Figure 5(a) shows experimental (curve with dots) and numerical (solid curve) magneto-optical response spectra for the sample under study. The magneto-optical response is calculated as $[T(H) - T(0)]/T(0)$, where T is the transmittance and H is the applied external magnetic field. To confirm our experimental results, we calculate the transmittance and magneto-optical response spectra [see Fig. 5(b)]. The mismatch between calculated and experimental spectra of the MO response can be explained by non-ideality of the experimental sample and convergence of incoming beam in the experiment comparing to a normal incidence of a plane wave in calculations. These factors lead to averaging of the optical signal,
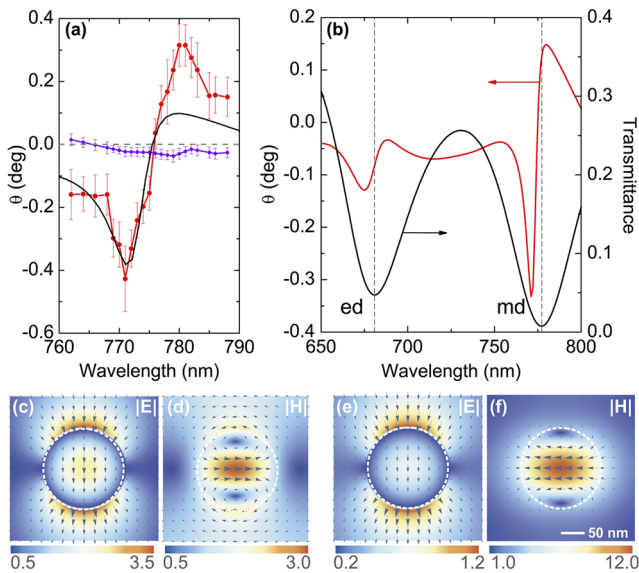
FIG. 3. (a) Experimental (red, dots) and numerical (black, solid) Faraday rotation spectra. The purple curve illustrates the experimentally measured Faraday rotation response of the reference nickel film; (b) Calculated transmittance (black curve) and Faraday effect (red curve) spectra; calculated local electric [(c) and (e)] and magnetic [(d) and (f)] fields inside the Si nanodisk in the vicinity of the electric dipole [(c) and (d)] and magnetic dipole [(e) and (f)] Mie-type resonances at λ = 675 nm and λ = 770 nm, respectively.
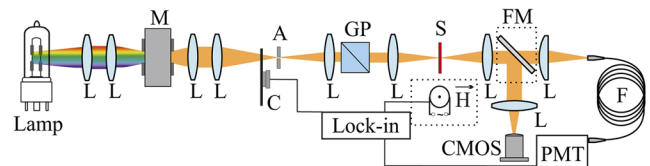
FIG. 4. Experimental setup for MO spectroscopy in Voigt configuration. The light source is a halogen lamp; L—lenses; M—monochromator; C—chopper; A—aperture; GP—Glan-Taylor polarizer; H—alternating magnetic field source; S—sample; FM—flipping mirror; CMOS—camera; F—multimode optical fiber; and PMT—photomultiplier tube.
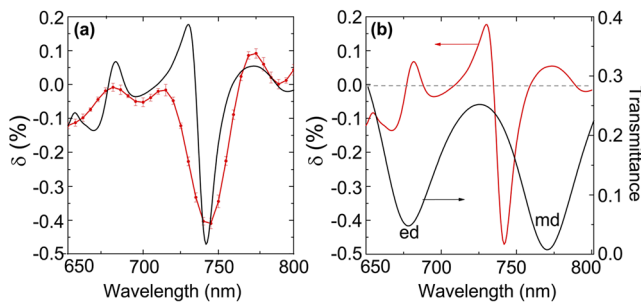
FIG. 5. (a) Experimental (red, dots) and numerical (black, solid) magneto-optical response measured in Voigt configuration; (b) Numerically calculated transmission (black curve) and magneto-optical response spectra (red curve) for the metasurface sample.

broadening of resonances in the experiment, and changes in the MO response as a consequence.

The contribution to the MO enhancement in case of electric dipole resonance is several times less than for the magnetic dipole resonance. Magneto-optical effects are susceptible to the mode character. Note that the MO Voigt effect corresponds to the first spectral derivative of the transmittance and thus does not coincide with a dip in the transmittance spectrum but matches with the maximal slope of the resonance curve. On the contrary, the Faraday effect reaches the maximum in the resonance, where the effective time of interaction between the incoming electromagnetic radiation and the resonant media is significantly increased, which mimics the gain in the magnetic layer with the thickness raise.

In conclusion, we have demonstrated, both experimentally and numerically, the multifold enhancement of the magneto-optical response both in Faraday and Voigt configurations in the spectral vicinity of the magnetic dipole Mie-type resonance of Si nanoparticles covered with a thin magnetic film. The characteristic values of the magneto-optical responses observed are $\theta = 0.8°$ and $\delta = 0.5\%$. It is noteworthy that the Faraday rotation angle switches up to 1° with the sign change on the ultranarrow (10 nm) spectral range in the vicinity of the optical magnetic resonance of the structure. It is a remarkable effect for the ultrathin magnetic material with the thickness of the only 5 nm. Specific Faraday rotation is $160°/\mu\text{m}$. These results can be potentially promising for ultrafast magnetophotonic metadevices.

APPENDIX A: NUMERICAL SIMULATIONS

The finite-difference time-domain method in the Lumerical FDTD Solutions software is used to calculate the optical response of the sample. The material dispersion data for amorphous silicon are taken from our ellipsometry measurements. The complex dielectric permittivity of the Ni film and glass substrate as a function of frequency is taken from the standard dispersion data.[47] The transmittance spectrum of the sample is calculated with using the model of a periodic array of silicon disks covered with a 5-nm-thick Ni film and placed on a semi-infinite glass substrate, illuminated at the normal incidence by a plane wave, polarized perpendicularly to the direction of magnetization. The periodic boundary conditions along both x- and y-axis and perfectly matched layers (PML) on the top and bottom of the unit cell to prevent parasitic interference are used. To obtain the magneto-optical response spectra, the non-diagonal complex permittivity tensor of the Ni film is taken into account.[46] The MO response in Voigt configuration is defined as $2 \cdot [T(H) - T(0)]/T(0)$, where T is the transmittance and H is the external magnetic field. The Faraday rotation effect is defined as $\theta = \arctan(E_x/E_y) \cdot 180/\pi$, where E_x and E_y are the x- and y-components of an electric field of the transmitted light. More detailed description of the numerical simulations can be found in Supporting Information of Ref. 21.

APPENDIX B: OPTICAL ROTATION POLARIMETRY

The Faraday rotation spectra are measured with a polarization-sensitive technique (see Fig. 2). A photoelastic modulator (PEM) is used as the analyzer for measuring the rotation of the polarization plane. The first polarizer after the laser is set in precise alignment with the retardation axis of the PEM. For this configuration, if there is no sample placed in the scheme, the AC component of the signal is absent, but there is a DC component. When a sample is inserted, the polarization rotation of the transmitted light is turned, and the photodetector registers the signal at the doubled frequency of the modulator. This signal is used to measure the rotation of the polarization plane. The signal at the detector is[48]

$$I(t) = \frac{1}{2}[1 - \sin(2\theta)\cos(\Delta_t)], \quad \text{(B1)}$$

where θ is the optical rotation and Δ_t is the time delay variation of the PEM. The detector signal can be rewritten in terms of Bessel functions, and the ratio of DC (V_{DC}) and AC (V_{2f}) terms in the small angle approximation $\theta < 15°$ leads to the expression for the optical rotation,[48]

$$\theta(\text{deg}) = 46.91\frac{V_{2f}}{V_{DC}}. \quad \text{(B2)}$$

APPENDIX C: FABRICATION OF SAMPLES

The sample of the hybrid Ni-Si metasurfaces was made using a combination of the following techniques. First, a thin (220 nm) film of hydrogenated amorphous silicon (a-Si:H) was deposited onto a glass substrate by plasma-enhanced

chemical vapor deposition from the mixture of SiH_4 and He gases in Oxford PlasmaLab System 100. The thickness and the optical quality of the created films were measured by the J.A. Woollam Co. Spectroscopic Ellipsometer M-2000D. Positive tone ZEP-520 electron beam resist was then spin-coated over the film and exposed in the electron-beam lithography system (Raith 150). Then, after the development of the sample thin Cr film was deposited on top of it, and lift-off procedure was applied to achieve Cr hard mask on top of the a-Si:H film. Using the reactive ion etching technique, the Cr mask was transferred to the a-Si:H film in Oxford PlasmaLab System 100 with the mixture of SF_6 and CHF_3 gases. After that, the residual Cr was removed via wet etching to obtain pure silicon metasurfaces on the glass substrate. Finally, the sample was placed into the ATC-2400-V AJA magnetron sputter system, and the 5-nm-thick Ni layer was deposited on top of it covering both the silicon disks and the substrate.

REFERENCES

[1] J. McCord, "Progress in magnetic domain observation by advanced magneto-optical microscopy," J. Phys. D: Appl. Phys. **48**, 333001 (2015).

[2] L. Pitaevskii, E. Lifshitz, and J. Sykes, *Course of Theoretical Physics: Physical Kinetics* (Elsevier, 2017), Vol. 10.

[3] N. Yusuf, A. Rousan, and H. El-Ghanem, "The wavelength dependence of Faraday rotation in magnetic fluids," J. Appl. Phys. **64**, 2781–2782 (1988).

[4] B. Sepúlveda, J. González-Díaz, A. García-Martín, L. M. Lechuga, and G. Armelles, "Plasmon-induced magneto-optical activity in nanosized gold disks," Phys. Rev. Lett. **104**, 147401 (2010).

[5] Y. Li, Q. Zhang, A. V. Nurmikko, and S. Sun, "Enhanced magnetooptical response in dumbbell-like Ag–CoFe$_2$O$_4$ nanoparticle pairs," Nano Lett. **5**, 1689–1692 (2005).

[6] H. Uchida, Y. Masuda, R. Fujikawa, A. V. Baryshev, and M. Inoue, "Large enhancement of Faraday rotation by localized surface plasmon resonance in Au nanoparticles embedded in Bi: YIG film," J. Magn. Magn. Mater. **321**, 843–845 (2009).

[7] A. V. Chetvertukhin, A. I. Musorin, T. V. Dolgova, H. Uchida, M. Inoue, and A. A. Fedyanin, "Transverse magneto-optical Kerr effect in 2D gold–garnet nanogratings," J. Magn. Magn. Mater. **383**, 110–113 (2015).

[8] I. Zubritskaya, N. Maccaferri, X. Inchausti Ezeiza, P. Vavassori, and A. Dmitriev, "Magnetic control of the chiroptical plasmonic surfaces," Nano Lett. **18**, 302–307 (2017).

[9] V. Bonanni, S. Bonetti, T. Pakizeh, Z. Pirzadeh, J. Chen, J. Nogués, P. Vavassori, R. Hillenbrand, J. Åkerman, and A. Dmitriev, "Designer magnetoplasmonics with nickel nanoferromagnets," Nano Lett. **11**, 5333–5338 (2011).

[10] V. I. Belotelov, I. A. Akimov, M. Pohl, V. A. Kotov, S. Kasture, A. S. Vengurlekar, A. V. Gopal, D. R. Yakovlev, A. K. Zvezdin, and M. Bayer, "Enhanced magneto-optical effects in magnetoplasmonic crystals," Nat. Nanotechnol. **6**, 370–376 (2011).

[11] A. A. Grunin, A. G. Zhdanov, A. A. Ezhov, E. A. Ganshina, and A. A. Fedyanin, "Surface-plasmon-induced enhancement of magneto-optical Kerr effect in all-nickel subwavelength nanogratings," Appl. Phys. Lett. **97**, 261908 (2010).

[12] S. Sadeghi and S. M. Hamidi, "Enhanced Faraday rotation in one dimensional magneto-plasmonic structure due to Fano resonance," J. Magn. Magn. Mater. **451**, 305–310 (2018).

[13] J. F. Torrado, J. B. González-Díaz, M. U. González, A. García-Martín, and G. Armelles, "Magneto-optical effects in interacting localized and propagating surface plasmon modes," Opt. Express **18**, 15635–15642 (2010).

[14] M. Inoue, K. Arai, T. Fujii, and M. Abe, "One-dimensional magnetophotonic crystals," J. Appl. Phys. **85**, 5768–5770 (1999).

[15] S. Kahl and A. M. Grishin, "Enhanced Faraday rotation in all-garnet magneto-optical photonic crystal," Appl. Phys. Lett. **84**, 1438–1440 (2004).

[16] M. Levy and R. Li, "Polarization rotation enhancement and scattering mechanisms in waveguide magnetophotonic crystals," Appl. Phys. Lett. **89**, 121113 (2006).

[17] T. Goto, A. V. Dorofeenko, A. M. Merzlikin, A. V. Baryshev, A. P. Vinogradov, M. Inoue, A. A. Lisyansky, and A. B. Granovsky, "Optical Tamm states in one-dimensional magnetophotonic structures," Phys. Rev. Lett. **101**, 113902 (2008).

[18] T. Goto, A. V. Baryshev, M. Inoue, A. V. Dorofeenko, A. M. Merzlikin, A. P. Vinogradov, A. A. Lisyansky, and A. B. Granovsky, "Tailoring surfaces of one-dimensional magnetophotonic crystals: Optical Tamm state and Faraday rotation," Phys. Rev. B **79**, 125103 (2009).

[19] A. V. Baryshev, K. Kawasaki, P. B. Lim, and M. Inoue, "Interplay of surface resonances in one-dimensional plasmonic magnetophotonic crystal slabs," Phys. Rev. B **85**, 205130 (2012).

[20] M. N. Romodina, I. V. Soboleva, A. I. Musorin, Y. Nakamura, M. Inoue, and A. A. Fedyanin, "Bloch-surface-wave-induced Fano resonance in magnetophotonic crystals," Phys. Rev. B **96**, 081401 (2017).

[21] M. G. Barsukova, A. S. Shorokhov, A. I. Musorin, D. N. Neshev, Y. S. Kivshar, and A. A. Fedyanin, "Magneto-optical response enhanced by Mie resonances in nanoantennas," ACS Photonics **4**, 2390 (2017).

[22] K. Takahashi, F. Kawanishi, S. Mito, H. Takagi, K. Shin, J. Kim, P. Lim, H. Uchida, and M. Inoue, "Study on magnetophotonic crystals for use in reflection-type magneto-optical spatial light modulators," J. Appl. Phys. **103**, 07B331 (2008).

[23] N. Ansari, S. Khartsev, and A. Grishin, "Multicolor filter all-garnet magneto-optical photonic crystals," Opt. Lett. **37**, 3552–3554 (2012).

[24] J. Ballato and E. Snitzer, "Fabrication of fibers with high rare-earth concentrations for Faraday isolator applications," Appl. Opt. **34**, 6848–6854 (1995).

[25] A. A. Grunin, I. R. Mukha, A. V. Chetvertukhin, and A. A. Fedyanin, "Refractive index sensor based on magnetoplasmonic crystals," J. Magn. Magn. Mater. **415**, 72–76 (2016).

[26] B. Sepúlveda, A. Calle, L. M. Lechuga, and G. Armelles, "Highly sensitive detection of biomolecules with the magneto-optic surface-plasmon-resonance sensor," Opt. Lett. **31**, 1085–1087 (2006).

[27] T. Goto, R. Morimoto, J. W. Pritchard, M. Mina, H. Takagi, Y. Nakamura, P. B. Lim, T. Taira, and M. Inoue, "Magneto-optical Q-switching using magnetic garnet film with micromagnetic domains," Opt. Express **24**, 17635–17643 (2016).

[28] C. D. Stanciu, F. Hansteen, A. Kimel, A. Kirilyuk, A. Tsukamoto, A. Itoh, and T. Rasing, "All-optical magnetic recording with circularly polarized light," Phys. Rev. Lett. **99**, 047601 (2007).

[29] K. Vahaplar, A. Kalashnikova, A. Kimel, D. Hinzke, U. Nowak, R. Chantrell, A. Tsukamoto, A. Itoh, A. Kirilyuk, and T. Rasing, "Ultrafast path for optical magnetization reversal via a strongly nonequilibrium state," Phys. Rev. Lett. **103**, 117201 (2009).

[30] T. Liu, T. Wang, A. Reid, M. Savoini, X. Wu, B. Koene, P. Granitzka, C. Graves, D. Higley, Z. Chen *et al.*, "Nanoscale confinement of all-optical magnetic switching in TbFeCo-competition with nanoscale heterogeneity," Nano Lett. **15**, 6862–6868 (2015).

[31] A. Dutta, A. V. Kildishev, V. M. Shalaev, A. Boltasseva, and E. E. Marinero, "Surface-plasmon opto-magnetic field enhancement for all-optical magnetization switching," Opt. Mater. Express **7**, 4316–4327 (2017).

[32] A. I. Musorin, M. I. Sharipova, T. V. Dolgova, M. Inoue, and A. A. Fedyanin, "Ultrafast Faraday rotation of slow light," Phys. Rev. Appl. **6**, 024012 (2016).

[33] M. R. Shcherbakov, P. P. Vabishchevich, A. Y. Frolov, T. V. Dolgova, and A. A. Fedyanin, "Femtosecond intrapulse evolution of the magneto-optic Kerr effect in magnetoplasmonic crystals," Phys. Rev. B **90**, 201405 (2014).

[34] A. I. Kuznetsov, A. E. Miroshnichenko, M. L. Brongersma, Y. S. Kivshar, and B. Luk'yanchuk, "Optically resonant dielectric nanostructures," Science **354**, aag2472 (2016).

[35] A. Y. Zhu, A. I. Kuznetsov, B. Luk'yanchuk, N. Engheta, and P. Genevet, "Traditional and emerging materials for optical metasurfaces," Nanophotonics **6**, 452–471 (2017).

[36]A. Li, S. Singh, and D. Sievenpiper, "Metasurfaces and their applications," Nanophotonics **7**, 989–1011 (2018).

[37]S. B. Glybovski, S. A. Tretyakov, P. A. Belov, Y. S. Kivshar, and C. R. Simovski, "Metasurfaces: From microwaves to visible," Phys. Rep. **634**, 1–72 (2016).

[38]N. Yu, F. Aieta, P. Genevet, M. A. Kats, Z. Gaburro, and F. Capasso, "A broadband, background-free quarter-wave plate based on plasmonic metasurfaces," Nano Lett. **12**, 6328–6333 (2012).

[39]K. E. Chong, L. Wang, I. Staude, A. R. James, J. Dominguez, S. Liu, G. S. Subramania, M. Decker, D. N. Neshev, I. Brener, and Y. S. Kivshar, "Efficient polarization-insensitive complex wavefront control using Huygens' metasurfaces based on dielectric resonant meta-atoms," ACS Photonics **3**, 514–519 (2016).

[40]Y. F. Yu, A. Y. Zhu, R. Paniagua-Domínguez, Y. H. Fu, B. Luk'yanchuk, and A. I. Kuznetsov, "High-transmission dielectric metasurface with 2π phase control at visible wavelengths," Laser Photonics Rev. **9**, 412–418 (2015).

[41]M. R. Shcherbakov, S. Liu, V. V. Zubyuk, A. Vaskin, P. P. Vabishchevich, G. Keeler, T. Pertsch, T. V. Dolgova, I. Staude, I. Brener *et al.*, "Ultrafast all-optical tuning of direct-gap semiconductor metasurfaces," Nat. Commun. **8**, 17 (2017).

[42]J. Bohn, T. Bucher, K. E. Chong, A. Komar, D.-Y. Choi, D. N. Neshev, Y. S. Kivshar, T. Pertsch, and I. Staude, "Active tuning of spontaneous emission by Mie-resonant dielectric metasurfaces," Nano Lett. **18**, 3461–3465 (2018).

[43]M. Parry, A. Komar, B. Hopkins, S. Campione, S. Liu, A. E. Miroshnichenko, J. Nogan, M. B. Sinclair, I. Brener, and D. N. Neshev, "Active tuning of high-Q dielectric metasurfaces," Appl. Phys. Lett. **111**, 053102 (2017).

[44]A. I. Musorin, M. G. Barsukova, A. S. Shorokhov, B. S. Luk'yanchuk, and A. A. Fedyanin, "Manipulating the light intensity by magnetophotonic metasurfaces," J. Magn. Magn. Mater. **459**, 165 (2018).

[45]A. Christofi, Y. Kawaguchi, A. Alù, and A. B. Khanikaev, "Giant enhancement of Faraday rotation due to electromagnetically induced transparency in all-dielectric magneto-optical metasurfaces," Opt. Lett. **43**, 1838–1841 (2018).

[46]G. S. Krinchik and V. A. Artemjev, "Magneto-optic properties of nickel, iron, and cobalt," J. Appl. Phys. **39**, 1276–1278 (1968).

[47]E. D. Palik, *Handbook of Optical Constants of Solids* (Academic Press, Boston, 1985).

[48]See http://www.hindsinstruments.com for polarization-sensitive technique description.